Vaccine 37 (2019) 1897–1903

Contents lists available at ScienceDirect

Vaccine

journal homepage: www.elsevier.com/locate/vaccine

Improving immunogenicity of influenza virus H7N9 recombinant hemagglutinin for vaccine development

Ting-Hui-Lin [a,b], Min-Yuan Chia [a,c], Chun-Yang Lin [a], Yi-Qi Yeh [d], U-Ser Jeng [d,e], Wen-Guey Wu [b], Min-Shi Lee [a,*]

[a] National Institute of Infectious Diseases and Vaccinology, National Health Research Institutes, Zhunan, Miaoli County, Taiwan
[b] College of Life Science, National Tsing-Hua University, Hsinchu, Taiwan
[c] Department of Veterinary Medicine, National Chung Hsing University, Taichung, Taiwan
[d] National Synchrotron Radiation Research Center, Hsinchu, Taiwan
[e] Department of Chemical Engineering, National Tsing Hua University, Hsinchu, Taiwan

ARTICLE INFO

Article history:
Received 15 May 2018
Received in revised form 8 September 2018
Accepted 13 September 2018

Keywords:
H7N9
Hemagglutinin
Influenza vaccine
Transmembrane domain

ABSTRACT

Human infections of novel avian influenza A virus (H7N9) emerged in early 2013 and caused about 40% case-fatality through 2017. Therefore, development of influenza H7N9 vaccines is critical for pandemic preparedness. Currently, there are three means of production of commercial influenza vaccines: egg-based, mammalian cell-based, and insect cell-based platforms. The insect cell-based platform has the advantage of high speed in producing recombinant protein. In this study, we evaluate the stability and immunogenicity of two different influenza H7 HA expression constructs generated using the baculovirus system, including membrane-based full-length HA (mH7) and secreted ectodomain-based H7 (sH7). The mH7 construct could form an oligomer-rosette structure and had a high hemagglutinin (HA) titer 8192. In contrast to mH7, the sH7 construct could not form an oligomer-rosette structure and did not have HA titer before cross-linking with anti-His antibody. Thermal stability tests showed that the sH7 and mH7 constructs were unstable at 43 °C and 52 °C, respectively. In a mice immunization study, the mH7 construct but not the sH7 construct could induce robust HI and neutralizing antibody titers. In conclusion, further development of the mH7 vaccine candidate is desirable.

1. Introduction

In March 2013, the first human case of infection with the H7N9 avian influenza virus was reported in Shanghai. Before this outbreak, avian influenza viruses have sporadically infected humans [1,2]. As is well known, over the past hundred years four influenza viruses have adapted to human populations and become pandemic strains: H1N1 in 1918, H2N2 in 1957, H3N2 in 1968, and swine-origin H1N1 in 2009 [3–6]. To date, a series of H7N9 outbreaks has caused severe economic losses in the poultry market and led to 1566 laboratory-confirmed human cases (http://www.who.int/influenza/human_animal_interface/HAI_Risk_Assessment/en/). In Taiwan, four human cases of H7N9 immigrated from China were reported during the first- and second-wave outbreaks in 2013 and 2014, respectively [7,8]. An effective vaccine that can be produced faster than traditional egg-based vaccines is required help combat a possible pandemic.

Hemagglutinin (HA), a major surface protein of the influenza virus, is responsible for host recognition by binding to host receptors and is the major target for neutralizing antibodies; therefore, it is a crucial antigen for vaccine development [9]. This viral protein is synthesized as a monomer (HA0) and assembled into homotrimer from ER to Golgi and then retained on viral membrane by the transmembrane (TM) domain, which is composed of 25–28 amino acids [10]. Recently, several mutations in the TM domain were able to change the post-translational modification postulated to affect viral growth, infection, and HA distribution [11–14]. Therefore, it may influence maintaining protein conformation and be associated with lipid raft for effective virus replication [11,15]. However, a number of studies indicate that HA can still maintain a trimeric conformation in the absence of the TM domain [16,17].

There are two primary platforms for production of influenza vaccines. First, the traditional egg-based manufacturing process has been used to prepare seasonal influenza vaccine. For this,

* Corresponding author at: National Health Research Institutes R1-7F, No. 35 Keyan Road, Zhunan, Miaoli County 35053, Taiwan.
E-mail address: Minshi@nhri.org.tw (M.-S. Lee).

https://doi.org/10.1016/j.vaccine.2018.09.034
0264-410X/

high-yield virus strains need to be selected; and the vaccine production consumes numerous chicken embryonic eggs. This process takes many steps and requires about six months. Additionally, people who are allergic to eggs cannot receive this vaccine [18,19]. Second, cell-based technology has been seen as an attractive alternative for vaccine development. Although this system also needs high-yield virus strains to infect cells, the time required is much less than with egg-based systems, facilitating the making of vaccines available in a timely manner.

Because of antigenic drift in influenza viruses, vaccine strains must be changed annually, a time-consuming process [20]. Recombinant protein technology is safe and rapid, because it requires only the sequence of the target antigen without virus selection or reassortant. Several studies using animal models have indicated that the purified recombinant proteins and virus-like particles from the recombinant baculovirus system were able to induce a significant immune response [21–25]. However, in a mice study the recombinant H7 vaccines have been confirmed to induce lower neutralizing antibody than seasonal viruses [26]. Therefore, several pandemic H7N9 vaccines attempted to improve the antibody response by using different platforms [27–29].

In our study, we set up a baculovirus-expression system to express recombinant A/Taiwan/1/2013 (H7N9) hemagglutinin based on soluble (sH7) and a full-length hemagglutinin construct of H7 (mH7) to evaluate their structural stability, hemagglutination, and immunogenicity for pandemic H7N9 vaccine development.

2. Materials and methods

2.1. Recombinant HA construction

cDNA of A/Taiwan/1/2013 (H7N9) influenza virus was provided by Taiwan's Centers for Disease Control, and the hemagglutinin (HA) was amplified by polymerase chain reaction (PCR). This HA gene incorporated gp67 baculovirus signal peptide at the N-terminal and thrombin cleavage site, followed by foldon sequence from bacteriophage T4 fibritin for producing functional HA trimer and a hexa his-tag at C- terminal for purification (Fig. S1A, designated sH7) [9,30]. The full-length HA containing original signal peptides and transmembrane domain (Fig. S1B, designated mH7) was amplified with the corresponding enzyme-cutting site by PCR. Two modified HA genes were cloned into baculovirus transfer vector using pFastBac Dual (Invitrogen) and transformed into competent DH10Bac *E. coli* cells.

2.2. Baculovirus production

Recombinant sH7 and mH7 virus were generated using a Bac-to-Bac baculovirus expression system (Invitrogen) according to the manufacturer's instructions. Briefly, Spodoptera frugiperda (Sf21) cells were transfected with pFastBac-sH7 and pFastBac-mH7 using cellfectin II reagent. After plaque purification to insure clonality, the sH7 and mH7 stocks were prepared by infecting cells at a low multiplicity of infection (MOI) of 0.1 per cell and harvested after 6 days.

2.3. Expression and purification

For large-scale sH7 production, a suspension of Trichoplusia ni (Hi5) cells (Invitrogen) was cultured in a shaker flask and incubated at 28 °C to a cell density of 2×10^6 cells/ml. Cells were then infected with sH7 recombinant baculovirus at an MOI of 5 and incubated at 28 °C. The cultured suspensions were collected 60 to 68 h after infection, and clarified by centrifugation (2000*g*, 4 °C, 20 min). Soluble sH7 proteins were obtained from cell suspension by metal affinity chromatography using Ni Sepharose excel resin. After washing with 50 mM imidazole, the sH7 was eluted with elution buffer (10 mM Tris, 50 mM NaCl, 500 mM imidazole, pH 8) from Ni resin. The fraction containing sH7 protein was further purified by Mono Q 5/50 and superdex 200 increase 10/300 size-exclusion chromatography (SEC). Fractions containing trimeric HA were concentrated using Amicon Ultracell (Millipore) with a cutoff of 30 kDa.

For mH7 production, suspension Sf21 cells were cultured in a shaker flask to 2×10^6 cells/ml and infected at an MOI of 5. The infected cells were harvested by centrifugation (1000*g*, 4 °C, 10 min) after 60 h. Cell pellets were extracted in extraction buffer (1% NP-9, 5% glycerol, 20 mM phosphate, 1 mM EDTA, pH 5.8) using a magnetic stirrer at 4 °C for 20 min; they were further clarified by centrifugation (13,000*g*, 4 °C, 30 min). After centrifugation, clarified extraction buffer was loaded into Q/S chromatography column (GE Healthcare) and washed with a 2 column volume (CV) running buffer (0.01% NP-9, 5% glycerol, 20 mM phosphate, 1 mM EDTA, pH 5.8); HA was eluted in elution buffer (0.03% NP-9, 5% glycerol, 20 mM phosphate, pH 7.05) with 150 mM NaCl in S column [31].

2.4. Hemadsorption test

Sf21 cells were infected with baculovirus containing mH7 gene at an MOI of 3. The infected cells and non-infected cells were collected into 1.5 ml microtubes at 48 h, 54 h, 60 h, and 66 h, and incubated with 0.1 ml 0.5% turkey red blood cells (TKRBCs). After gentle mixing and incubation for 30 min, the reaction samples were loaded in 6-well plates and observed under a microscope.

2.5. Recombinant protein stability assay

In order to examine HA stability, the recombinant HA proteins were mixed with trypsin (Sigma T8802) at a final ratio of 1000:1 (wt/wt) in 20 mM Tris and 150 mM NaCl, pH8, and incubated at 20 °C for 16 h. These digestion mixtures were subsequently analyzed by SDS-PAGE.

To understand the thermal stability of HA, each recombinant protein (2 μg/well) was mixed with Sypro orange dye (final 1X) in reaction buffer (10 mM Tris, 100 mM NaCl, pH8) and added to a 96 well plate to analyze from 20 to 95 °C by step one plus Real-Time PCR [32]. Data from thermal stability were calculated and analyzed by protein thermal shift software (Thermo Fisher).

2.6. SDS-PAGE and Western blotting

Recombinant sH7, sH7-m (sH7-monomer, Fig. 1A), and mH7 were confirmed by SDS-PAGE and Western blotting in reducing condition using polyclonal goat anti-H7 antibody from the United Kingdom's National Institute for Biological Standards and Control (NIBSC 13/180) [33].

2.7. Circular dichroism assay

Recombinant sH7, sH7-m, and mH7 were diluted into 10 mM phosphate and 500 mM sodium fluoride at final concentration (0.1 μg/ml) to compare the structure and stability of each form of HA protein. CD spectra were collected from 260 to 180 nm on beamline BL04C at the National Synchrotron Radiation Research Center [34].

2.8. Small-angle X-ray scattering (SAXS)

SAXS data were collected at the 23A SWAXS endstation of the National Synchrotron Radiation Research Center [35], equipped with an on-line size-exclusion high pressure liquid

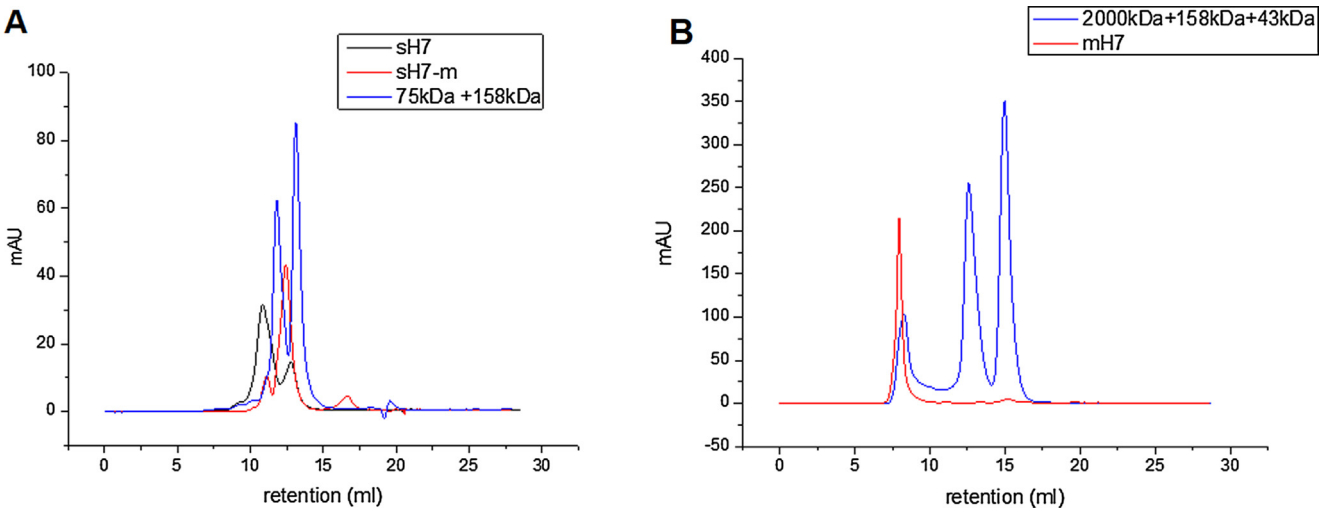

Fig. 1. Characterization of mH7 and sH7 using size exclusion chromatography. (A) Without the treatment of thrombin, the original sH7 (sH7-foldon) has trimer form (major peak, >158 kDa) and monomer forms (minor peak). After thrombin treatment, the foldon domain was removed and only monomer form was found (red line). (B) The purified mH7 is homogeneous with molecular about 2000 kDa. (For interpretation of the references to colour in this figure legend, the reader is referred to the web version of this article.)

chromatographic (SE-HPLC) system (Agilent chromatographic system 1260 series). Protein sample solutions, typically 50 μL with 5 mg mL^{-1}, were respectively injected into the HPLC column at a flow rate 0.4 ml/min. After SE-HPLC, the sample solution was directed into a quartz capillary (2 mm dia.) for SAXS measurements at 288 K. With UV–Vis absorption monitored at the SAXS sample position, data were collected successively with a rate of 1 frame per 30 s using a Pilatus 1 M-F area detector; frame data of identical profiles (i.e. no sign of radiation damage) were selectively combined (typically 5–10 frames) for improved statistics. Buffer solutions were measured under identical conditions for background scattering subtraction. With 15 keV X-rays (wavelength $\lambda = 0.8266$ Å) and a sample-to-detector distance of 3.2 m, the scattering vector q, defined by $4\pi\lambda^{-1}\sin\theta$ with a scattering angle of 2θ. Data were corrected for electronic noise, sample transmission, and detector sensitivity, followed by a scaling to absolute intensity $I(q)$ in units of cm^{-1} via scattering from water at the protein sample conditions [36,37].

Data were evaluated for radiation damage, background subtraction quality, and sample concentration effects; and well-overlapped SAXS profiles collected over the sample elution peak of HPLC were integrated for improved data statistics. Zero-angle scattering intensities (I_o) and the corresponding R_g values were extracted from SAXS data using the Guinier approximation. SAXS data evaluation and model fittings were performed using the ATSAS package. The distance distribution function $p(r)$ was Fourier transformed from the SAXS data; the corresponding maximum dimension D_{max} and Porod volumes were evaluated using GNOM [38,39]. Protein envelopes were obtained using SASREF software. A di-trimer was reconstructed via SASREF, based on the available crystal trimer structure PDB 4LN6 of HA [40]; a hierarchical rosette structure with 6-fold symmetry was then built from the di-trimer HA with refined relative orientation of the two trimers. CRYSOL was used in the SAXS data fitting with the available monomer crystal structure [38].

2.9. Animal vaccination

Female BALB/c mice were immunized intramuscularly with 3 doses of vaccine antigen at 2-week intervals. Four treatment groups (6 mice per group) immunized with vaccines containing different HA and adjuvant dosages were compared at weeks 0, 2, and 4, including (1) PBS 100 μL + 300 μg aluminum hydroxide (Al$(OH)_3$), (2) 20 μg sH7-m + 300 μg Al$(OH)_3$, (3) 1 μg sH7-m + 300 μg Al$(OH)_3$, and (4) 0.5 μg inactivated H7N9 whole virus vaccine + 300 μg Al$(OH)_3$. In another mice study with two doses of vaccination, three treatment groups were compared: (1) 20 μg mH7 + 300 μg Al$(OH)_3$, (2) 0.5 μg mH7 + 300 μg Al$(OH)_3$, and (3) 0.5 μg inactivated H7N9 whole virus vaccine + 300 μg Al$(OH)_3$. Blood was collected at 14 days post each immunization for measuring serum HI and neutralizing antibody titers.

2.10. Serological test

Sera from immunized mice were treated with receptor destroyed enzyme for 16 h at 37 °C, then heat inactivated for 30 min at 56 °C and diluted to a concentration of 1:10 in PBS. The titer of preimmunization sera were assigned to the <10 group (data not shown). Four HA units of inactivated virus (A/Taiwan/1/2013 (H7N9) virus) were added to each well with serums of two-fold serial dilution and incubated for 30 min at room temperature. An equal volume of 0.5% turkey RBC was added to each well and incubated for 30 min at room temperature. The HAI titer was read as the reciprocal of the highest dilution of serum that inhibited hemagglutination. Neutralizing antibody titers were detected using MDCK cells and were expressed as the reciprocal of the highest dilution of serum that gave 50% neutralization of 100 $TCID_{50}$ of the vaccine virus (A/Anhui/1/2013) following the WHO standard protocols [41].

2.11. Soluble hemagglutination assay

Soluble recombinant HA assay was carried out with monoclonal anti-his antibody. First, the sHA trimer containing his tag was premixed with anti-his in 2:1 (molar ratio) for 45 min. The mixture (sH7-antiHis) was transferred to a 96-well plate and reacted with turkey red blood cell for 30 min.

3. Results

3.1. Construction and identification of HA expressed in insect cells

Two different constructs were designed to express sH7 and mH7 (Fig. S1A and B). We first expressed trimeric soluble sH7,

which was incorporated with trimerization domain at N-terminal. At 60 h, supernatant was harvested and loaded into metal chromatography. After purification, the sH7 had one major band about 200 kDa and one minor band about 65 kDa (Fig. 1A, black line) but could not maintain trimer form after thrombin digestion (sH7-m) (Fig. 1A, red line). In SDS-PAGE analysis, the sH7 and sH7-m had one significant band (HA0) before trypsin treatment (Fig. S2A). After trypsin digestion, HA0 was cleaved into HA1 and three uniform HA2 (Fig. S2A), which were confirmed using Western blot (Fig. S2B). Although soluble HAs were produced in the baculovirus system and were studied in several crystallographic studies with natural trimer states, they cannot be detected with HA titer (Table1) [9,42].

For mH7 expression, infected cell pellets were harvested and the expression of HA protein on cell membrane was detected in about 90% of cell using hemadsorption; then the HA protein was extracted and purified using sequential chromatography from cell membrane. After purification using size exclusion chromatography, mH7 had high purity and a molecular weight of about 2000 kDa (Fig. 1B). The mH7-containing TM domain was expressed in oligomer form with high molecular weight and reacted with turkey RBC at an extremely high HA titer of 8192 (Table 1). In the SDS-PAGE analysis, we found mH7 had one major band (HA0, 65 kDa) without trypsin treatment. Interestingly, mH7 was cleaved into multiple size smaller than HA1 after trypsin treatment, which was confirmed using Western blot assay (Fig. S2B).

3.2. Structural stability of H7 protein in protease and thermal treatment

HA is synthesized as a HA0 and cleaved into HA1 and HA2 by host protease upon virus infection and release [43]. When HA are expressed in the baculovirus system, low pathogenic influenza retains its HA0 state [44,45]. In order to assess the structural stability of mH7, sH7, and sH7-m, the purified protein was analyzed by SDS-PAGE and Western blot following trypsin digestion.

After storage at 4 °C for one month, the sH7-m became heterogeneous before trypsin treatment and the HA1 was not predominant after trypsin treatment (Fig. S2C) findings confirmed by Western blot (Fig. S2D). In contrast, mH7 still maintained the same profile in the same storage scenario. Although mH7 was more sensitive to protease digestion at first, the secondary structure of mH7 seemed to have no significant differences with sH7 and sH7-m (Fig. S3). In thermal stability, sH7 and sH7-m dissolved at 43 °C and 41 °C, whereas the mH7-containing TM domain did not dissolve until 52 °C (Fig. S4). In addition, sH7 and sH7-m were also found second melting point at 53 °C and 55 °C (Fig. S4). This result was consistent with trypsin digestion, in which sH7 and sH7-m were more unstable.

3.3. Characterization of recombinant mH7 by small angle X-ray scattering

Based on size exclusion chromatography, the mH7 expressed in our baculovirus system appeared to be comprised of 12 trimers. We further used SAXS to extract a consistent rosette structure of mH7 of six-fold symmetry formed from 6 pairs of di-trimers. As shown in Fig. 2, the rosette conformations of the HA were reconstructed from the HPLC/SAXS data collected along the elution, revealing a small size distribution (radius of gyration Rg ranging from 118 to 130 Å), presumably the result of fluctuations of the rosette conformation. The corresponding population distribution is proportional to the zero-angle intensity $I(0)$ of SAXS.

3.4. Antibody responses

In order to compare the immunogenicity elicited from different HAs, mice were immunized with 1 μg and 20 μg of sH7-m, and 0.5 μg of inactivated H7 virus with 300 μg adjuvant. Sera were collected at 2 weeks post each immunization. The inactivated H7 virus was incubated with antisera from immunized mice to assess HI titer. In addition, the neutralization ability of antisera was evaluated in MDCK cells using A/Anhui/1/2013 H7N9 virus. The results indicated that mice immunized with inactivated virus elicited significant HI (Fig. 3A) and NT (Fig. 3B) titer at the second (HI GMT = 359, NT GMT = 452) and third immunizations (HI GMT = 2031, NT GMT = 1612). However, mice that received 20 μg of sH7-m elicited higher titer at the third immunization (GMT = 403); but the titer of the other group immunized with 1 μg of sH7 was still much lower (GMT = 40).

The mH7 was also tested with two different dosages (0.5 μg and 20 μg). Consistent with 1 μg dosage of sH7, the 0.5 μg dosage of mH7 induced low HI and NT titer at the first and second immunizations. With the 20 μg dosage of mH7, mice induced significant antibody titer in HI (Fig. 4A, GMT = 101), and the neutralizing ability of the sera to live virus to was observed with the NT titer higher (Fig. 4B, GMT = 114) than those of sH7 group (20 μg, GMT = 25; 1 μg, GMT = 12) after the second immunization.

4. Discussion

Avian influenza H7N9 virus has circulated globally and caused more than 1600 cases of human infection since 2013. Therefore, it is necessary to develop an influenza H7N9 vaccine for pandemic preparedness. Multiple platforms have been developed for production of influenza vaccines, including egg-derived, mammalian cell-derived, and insect cell-derived production platforms. Among them, the insect cell-derived platform has the following major advantages: it has a lower biosafety requirement and is easy to scale-up [46]. We focused on the development of influenza H7N9 vaccines using the insect cell-derived platform. Two types of recombinant protein have been generated, including sHA and mHA; but the immunogenicity of these two HA proteins has not been compared simultaneously. Since sHA containing foreign peptides (foldon and His-tag) is not suitable for human vaccines, the foldon domain needs to be removed. In our study, the sH7 dissociated into monomer (sH7-m) upon removal of the foldon domain through proteolytic cleavage with thrombin. Moreover, this sH7-m was unstable at 4 °C and has lower immunogenicity after a second boost in mice. This phenomenon was also observed in the rHA of A/Shanghai/1/2013 (H7N9) and A/Shanghai/2/2013 [40]. Interestingly, the recombinant H5 protein could maintain trimer conformation and have good immunogenicity in mice after removing the foldon domain [47].

To improve the immunogenicity of recombinant H7 protein, we generated the second construct containing the TM domain to have

Table 1
Hemagglutination (HA) titers of different influenza H7N9 antigens.

	Inactivated virus	Negative control[a]	sH7	sH7-anti-His	mH7
HA titer	128	<8	<8	16	8192

[a] Negative control: PBS + Anti-His.

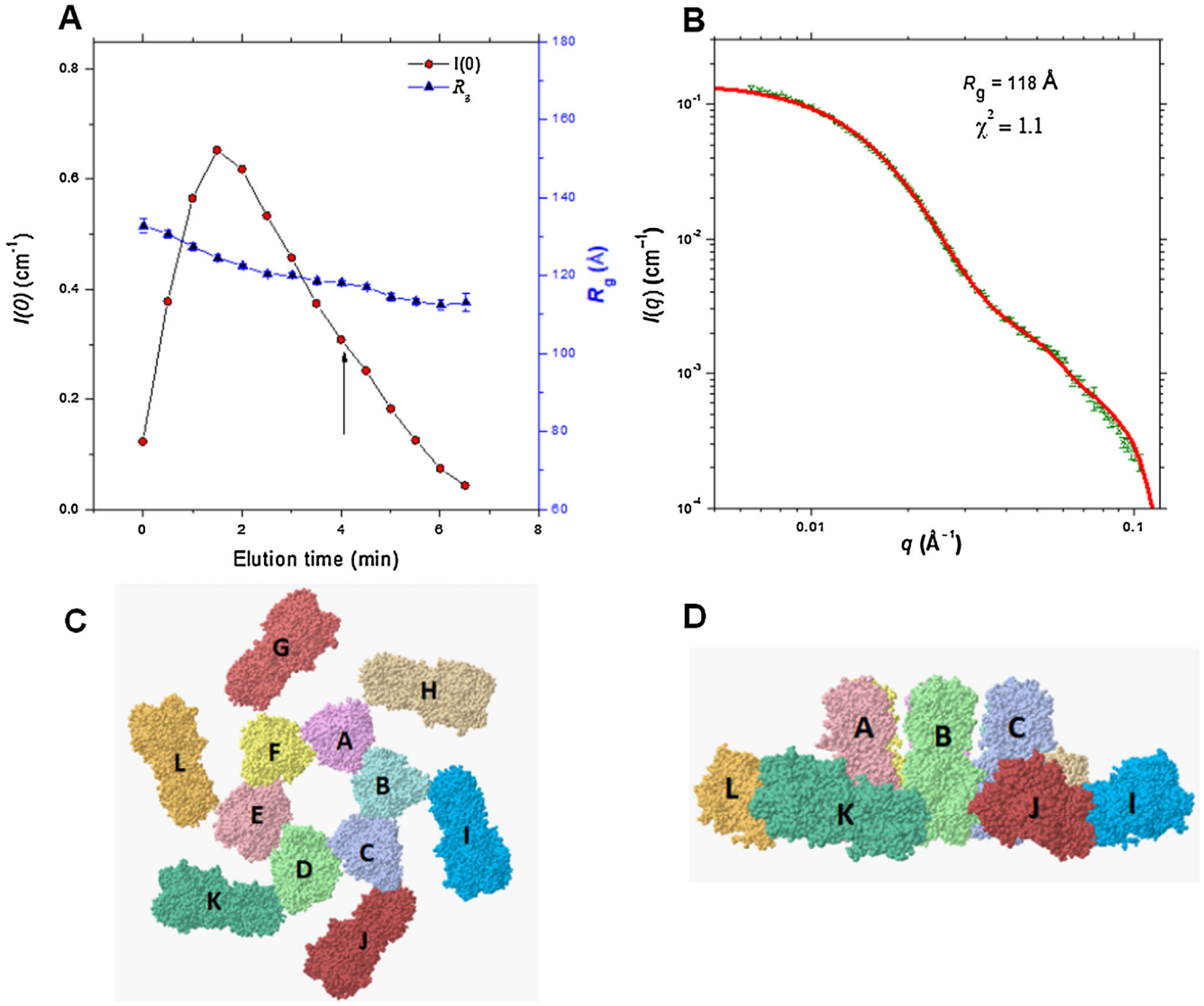

Fig. 2. HPLC/SAXS intensity and the evolution of the radius of gyration (R_g) and the corresponding rosette conformations (as shown) extracted along the sample elution time. (A) A typical set of SAXS data collected at t = 4 min, as indicated by an arrow, fitted using the SASREF protocol. (C) Side and (D) top views of an HA rosette of 6-fold symmetry reconstructed from the SAXS data in (B), using 6 di-trimers, with each trimer marked subsequently from A to K. Each of the di-trimers (e.g. A-H, B-I, or C-J) shares a common incline angle of ca. 90° between the two rod-like HA trimers. The hydrophobic sides of the di-trimers are closely associated with stabilization of the 6-fold rosette aggregation in solution.

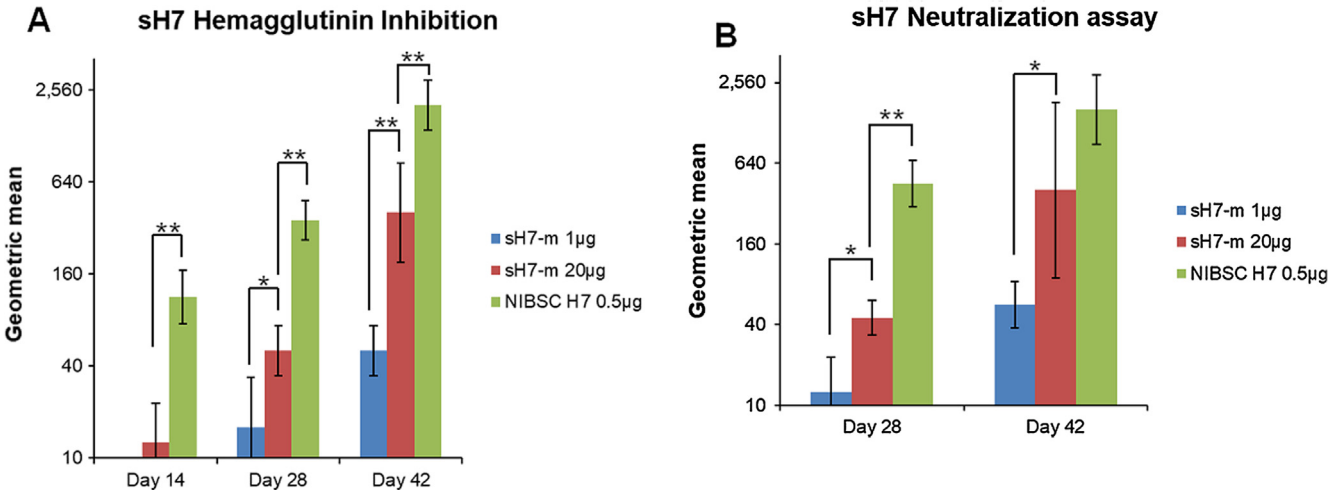

Fig. 3. Hemagglutinin inhibition and neutralization titers in mice immunized with egg-derived influenza H7N9 whole virus antigen (NIBSC H7N9) and recombinant influenza H7N9 HA monomer (sH7-m). Three immunizations were given at days 0, 14, and 28 with two different dosages (1 and 20 μg). Sera were collected at days 14, 28, and 42 for measuring HI (A) and NT (B) antibody titer. Statistically significant differences are indicated by * ($0.0001 < P < 0.05$) or ** ($P < 0.0001$).

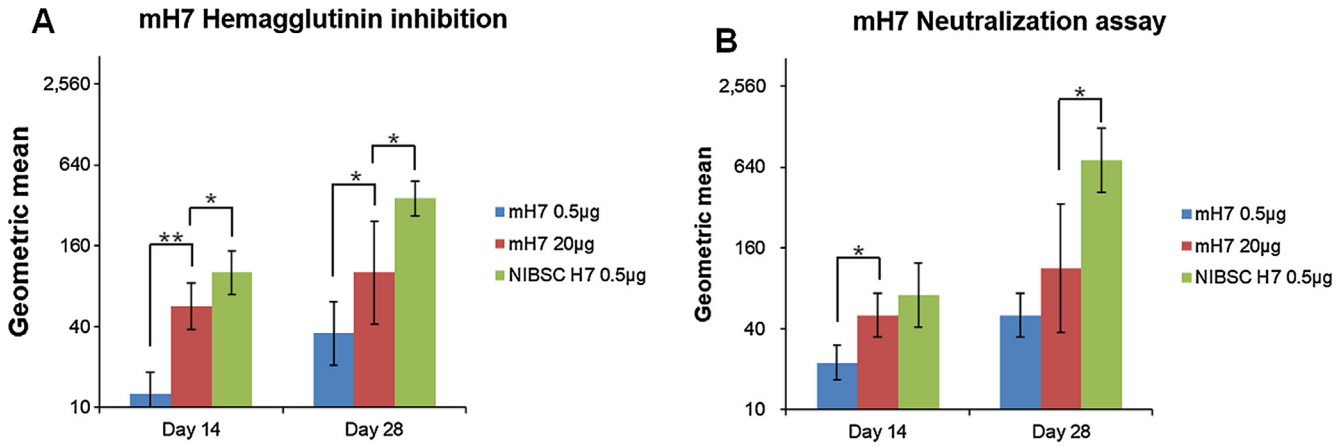

Fig. 4. Hemagglutinin inhibition and neutralization titers in mice immunized with egg-derived influenza H7N9 whole virus antigen (NIBSC H7N9) and recombinant influenza H7N9 membrane-based HA (mH7). Two immunizations recombinant HA protein were given at days 0 and 14; and sera with two different dosages (0.5 and 20 μg) were collected at days 14 and 28 for measuring HI (A) and NT (B) antibody titer. Statistically significant differences are indicated by * ($0.0001 < P < 0.05$) or ** ($P < 0.0001$).

an oligomer format. Oligomerization can enhance the extensive budding, replication, fusion, and structural stability of the virus [48,49]. Certain amino acid substitution at the TM domain leads to dissociation between HA and lipid raft, and also interrupts distribution of HA to form high order conformation on the virus surface [12,50]. Several studies have indicated that substituted redundant Cys with other amino acids in the TM domain and cytoplasmic tail can reduce undesirable cross-linked disulfide bonds and improve structural stability and immunogenicity [51]. In our study, the mH7 proteins carry only one cysteine residue in the TM domain and have better stability and higher immunogenicity compared with sH7-m. Previous studies indicate that recombinant HA containing TM domain in the solid phase can be observed in rosette states under cryo-EM [43,51]. We employed the solution SAXS with integrated on-line high performance liquid chromatography (HPLC-SAXS) to confirm that mH7 in natural phase can form into highly ordered rosettes, with six pairs of di-timers (Fig. 2). Secondary structure among sH7, sH7-m, and mH7 did not show significant differences in the CD data. The stability of H7 HA might be influenced by intermolecular force. This phenomenon has described in H1N1 HA, which was found an amino acid substitution can affect the structure stability [33]. However, the oligomerization seems to be a critical force that can maintain structural stability. According to this concept, the sH7-antihis complex was observed with HA titer might form oligomerization of sH7 and anti-His antibody complex. Overall, recombinant HA forming into oligomer rosettes could have better stability and immunogenicity.

The baculovirus platform has also been used to develop other H7N9 vaccines, such as recombinant virus-like particles (VLP) [23,52]. The H7N9 VLP vaccine candidate completed phase one clinical trials less than six months after the H7N9 outbreak was reported [52]. Therefore, the baculovirus platform has the advantage of high speed to develop influenza vaccines for pandemic preparedness.

Acknowledgments

We thank Dr. Yung-Chih Alan Hu and Dr. Wang-Chou Sung at the National Health Research Institutes for providing purification facilities, Mark Swofford for English editing, and Dr. Chang-Chun David Lee at Academia Sinica for discussion. Ting-Hui Lin carried out his thesis research under the auspices of the Graduate Program of Biotechnology in Medicine, NTHU and NHRI in acknowledgement.

Funding

We appreciate funding from the Ministry of Science and Technology (106-3114-Y404-002) and the National Health Research Institutes.

Conflict of interest statement

All authors declare that they have no conflicts of interest in this study.

Appendix A. Supplementary material

Supplementary data to this article can be found online at https://doi.org/10.1016/j.vaccine.2018.09.034.

References

[1] Watanabe T, Watanabe S, Maher EA, Neumann G, Kawaoka Y. Pandemic potential of avian influenza A (H7N9) viruses. Trends Microbiol 2014;22:623–31.
[2] Gao R, Cao B, Hu Y, Feng Z, Wang D, Hu W, et al. Human infection with a novel avian-origin influenza A (H7N9) virus. New England J Med 2013;368:1888–97.
[3] Kawaoka Y, Bean WJ, Webster RG. Evolution of the hemagglutinin of equine H3 influenza viruses. Virology 1989;169:283–92.
[4] Reid AH, Fanning TG, Hultin JV, Taubenberger JK. Origin and evolution of the 1918 "Spanish" influenza virus hemagglutinin gene. PNAS 1999;96:1651–6.
[5] Scholtissek C, Rohde W, Von Hoyningen V, Rott R. On the origin of the human influenza virus subtypes H2N2 and H3N2. Virology 1978;87:13–20.
[6] Smith GJD, Vijaykrishna D, Bahl J, Lycett SJ, Worobey M, Pybus OG, et al. Origins and evolutionary genomics of the 2009 swine-origin H1N1 influenza A epidemic. Nature 2009;459:1122–5.
[7] Yang JR, Kuo CY, Huang HY, Wu FT, Huang YL, Cheng CY, et al. Characterization of influenza A (H7N9) viruses isolated from human cases imported into Taiwan. PLoS One 2015;10:e0119792.
[8] Chang SY, Lin PH, Tsai JC, Hung CC, Chang SC. The first case of H7N9 influenza in Taiwan. Lancet (London, England) 2013;381:1621.
[9] Stevens J, Corper AL, Basler CF, Taubenberger JK, Palese P, Wilson IA. Structure of the uncleaved human H1 hemagglutinin from the extinct 1918 influenza virus. Science 2004;303:1866–70.
[10] Kordyukova L. Structural and functional specificity of Influenza virus haemagglutinin and paramyxovirus fusion protein anchoring peptides. Virus Res 2017;227:183–99.
[11] Takeda M, Leser GP, Russell CJ, Lamb RA. Influenza virus hemagglutinin concentrates in lipid raft microdomains for efficient viral fusion. PNAS 2003;100:14610–7.
[12] Rossman JS, Lamb RA. Influenza virus assembly and budding. Virology 2011;411:229–36.
[13] Chen BJ, Takeda M, Lamb RA. Influenza virus hemagglutinin (H3 subtype) requires palmitoylation of its cytoplasmic tail for assembly: M1 proteins of two subtypes differ in their ability to support assembly. J Virol 2005;79:13673–84.

[14] Zhang J, Pekosz A, Lamb RA. Influenza virus assembly and lipid raft microdomains: a role for the cytoplasmic tails of the spike glycoproteins. J Virol 2000;74:4634–44.
[15] Tall RD, Alonso MA, Roth MG. Features of influenza HA required for apical sorting differ from those required for association with DRMs or MAL. Traffic (Copenhagen, Denmark) 2003;4:838–49.
[16] Yang H, Carney PJ, Donis RO, Stevens J. Structure and receptor complexes of the hemagglutinin from a highly pathogenic H7N7 influenza virus. J Virol 2012;86:8645–52.
[17] Lin SC, Huang MH, Tsou PC, Huang LM, Chong P, Wu SC. Recombinant trimeric HA protein immunogenicity of H5N1 avian influenza viruses and their combined use with inactivated or adenovirus vaccines. PLoS One 2011;6:e20052.
[18] Wood JMaW, M.S. History of inactivated influenza vaccines; 1998.
[19] Partridge J, Kieny MP. Global production of seasonal and pandemic (H1N1) influenza vaccines in 2009–2010 and comparison with previous estimates and global action plan targets. Vaccine 2010;28:4709–12.
[20] Wood JM. Selection of influenza vaccine strains and developing pandemic vaccines. Vaccine 2002;20(Suppl 5):B40–4.
[21] Cox MM, Hollister JR. FluBlok, a next generation influenza vaccine manufactured in insect cells. Biol: J Int Assoc Biol Stand 2009;37:182–9.
[22] Treanor JJ, Betts RF, Smith GE, Anderson EL, Hackett CS, Wilkinson BE, et al. Evaluation of a recombinant hemagglutinin expressed in insect cells as an influenza vaccine in young and elderly adults. J Infect Dis 1996;173:1467–70.
[23] Liu YV, Massare MJ, Pearce MB, Sun X, Belser JA, Maines TR, et al. Recombinant virus-like particles elicit protective immunity against avian influenza A(H7N9) virus infection in ferrets. Vaccine 2015;33:2152–8.
[24] Izikson R, Leffell DJ, Bock SA, Patriarca PA, Post P, Dunkle LM, et al. Randomized comparison of the safety of Flublok® versus licensed inactivated influenza vaccine in healthy, medically stable adults ≥50 years of age. Vaccine 2015;33:6622–8.
[25] Cox MM, Izikson R, Post P, Dunkle L. Safety, efficacy, and immunogenicity of Flublok in the prevention of seasonal influenza in adults. Therap Adv Vacc 2015;3:97–108.
[26] Blanchfield K, Kamal RP, Tzeng WP, Music N, Wilson JR, Stevens J, et al. Recombinant influenza H7 hemagglutinins induce lower neutralizing antibody titers in mice than do seasonal hemagglutinins. Influenza Other Respir Viruses 2014;8:628–35.
[27] Kamal RP, Blanchfield K, Belser JA, Music N, Tzeng WP, Holiday C, et al. Inactivated H7 Influenza virus vaccines protect mice despite inducing only low levels of neutralizing antibodies. J Virol 2017;91.
[28] Klausberger M, Wilde M, Palmberger D, Hai R, Albrecht RA, Margine I, et al. One-shot vaccination with an insect cell-derived low-dose influenza A H7 virus-like particle preparation protects mice against H7N9 challenge. Vaccine 2014;32:355–62.
[29] Kreijtz JHCM, Wiersma LCM, De Gruyter HLM, Vogelzang-van Trierum SE, van Amerongen G, Stittelaar KJ, et al. A single immunization with modified vaccinia virus ankara–based influenza virus H7 vaccine affords protection in the Influenza A(H7N9) pneumonia ferret model. J Infect Dis 2015;211:791–800.
[30] Frank S, Kammerer RA, Mechling D, Schulthess T, Landwehr R, Bann J, et al. Stabilization of short collagen-like triple helices by protein engineering. J Mol Biol 2001;308:1081–9.
[31] Wang K, Holtz KM, Anderson K, Chubet R, Mahmoud W, Cox MM. Expression and purification of an influenza hemagglutinin–one step closer to a recombinant protein-based influenza vaccine. Vaccine 2006;24:2176–85.
[32] Grøftehauge MK, Hajizadeh NR, Swann MJ, Pohl E. Protein–ligand interactions investigated by thermal shift assays (TSA) and dual polarization interferometry (DPI). Acta Crystallogr D Biol Crystallogr 2015;71:36–44.
[33] Yang H, Chang JC, Guo Z, Carney PJ, Shore DA, Donis RO, et al. Structural stability of influenza A(H1N1)pdm09 virus hemagglutinins. J Virol 2014;88:4828–38.
[34] Liu SH, Lin YH, Huang LJ, Luo SW, Tsai WL, Chiang SY, et al. Design and construction of a compact end-station at NSRRC for circular-dichroism spectra in the vacuum-ultraviolet region. J Synchrotron Radiat 2010;17:761–8.
[35] Jeng U-S, Su CH, Su C-J, Liao K-F, Chuang W-T, Lai Y-H, et al. A small/wide-angle X-ray scattering instrument for structural characterization of air-liquid interfaces, thin films and bulk specimens. J Appl Crystallogr 2010;43:110–21.
[36] Yeh YQ, Liao KF, Shih O, Shiu YJ, Wu WR, Su CJ, et al. Probing the acid-induced packing structure changes of the molten globule domains of a protein near equilibrium unfolding. J Phys Chem Lett 2017;8:470–7.
[37] Shih O, Yeh YQ, Liao KF, Sung TC, Chiang YW, Jeng US. Oligomerization process of Bcl-2 associated X protein revealed from intermediate structures in solution. Phys Chem Chem Phys 2017;19:7947–54.
[38] Petoukhov MV, Franke D, Shkumatov AV, Tria G, Kikhney AG, Gajda M, et al. New developments in the ATSAS program package for small-angle scattering data analysis. J Appl Crystallogr 2012;45:342–50.
[39] Petoukhov MV, Svergun DI. Global rigid body modeling of macromolecular complexes against small-angle scattering data. Biophys J 2005;89:1237–50.
[40] Yang H, Carney PJ, Chang JC, Villanueva JM, Stevens J. Structural analysis of the hemagglutinin from the recent 2013 H7N9 influenza virus. J Virol 2013;87:12433–46.
[41] WHO. World Health Organization. WHO manual on animal influenza diagnosis and surveillance Geneva: WHO; 2002. July 12.
[42] Stevens J, Blixt O, Tumpey TM, Taubenberger JK, Paulson JC, Wilson IA. Structure and receptor specificity of the hemagglutinin from an H5N1 influenza virus. Science 2006;312:404–10.
[43] Bottcher C, Ludwig K, Herrmann A, van Heel M, Stark H. Structure of influenza haemagglutinin at neutral and at fusogenic pH by electron cryo-microscopy. FEBS Lett 1999;463:255–9.
[44] Kuroda K, Hauser C, Rott R, Klenk HD, Doerfler W. Expression of the influenza virus haemagglutinin in insect cells by a baculovirus vector. EMBO J 1986;5:1359–65.
[45] Crawford J, Wilkinson B, Vosnesensky A, Smith G, Garcia M, Stone H, et al. Baculovirus-derived hemagglutinin vaccines protect against lethal influenza infections by avian H5 and H7 subtypes. Vaccine 1999;17:2265–74.
[46] van Oers MM, Pijlman GP, Vlak JM. Thirty years of baculovirus-insect cell protein expression: from dark horse to mainstream technology. J Gen Virol 2015;96:6–23.
[47] Wei CJ, Xu L, Kong WP, Shi W, Canis K, Stevens J, et al. Comparative efficacy of neutralizing antibodies elicited by recombinant hemagglutinin proteins from avian H5N1 influenza virus. J Virol 2008;82:6200–8.
[48] Buckland B, Boulanger R, Fino M, Srivastava I, Holtz K, Khramtsov N, et al. Technology transfer and scale-up of the Flublok recombinant hemagglutinin (HA) influenza vaccine manufacturing process. Vaccine 2014;32:5496–502.
[49] Feshchenko E, Rhodes DG, Felberbaum R, McPherson C, Rininger JA, Post P, et al. Pandemic influenza vaccine: characterization of A/California/07/2009 (H1N1) recombinant hemagglutinin protein and insights into H1N1 antigen stability. BMC Biotech 2012;12:77.
[50] Leser GP, Lamb RA. Lateral organization of influenza virus proteins in the budozone region of the plasma membrane. J Virol 2017;91.
[51] Holtz KM, Robinson PS, Matthews EE, Hashimoto Y, McPherson CE, Khramtsov N, et al. Modifications of cysteine residues in the transmembrane and cytoplasmic domains of a recombinant hemagglutinin protein prevent cross-linked multimer formation and potency loss. BMC Biotech 2014;14:111.
[52] Smith GE, Flyer DC, Raghunandan R, Liu Y, Wei Z, Wu Y, et al. Development of influenza H7N9 virus like particle (VLP) vaccine: homologous A/Anhui/1/2013 (H7N9) protection and heterologous A/chicken/Jalisco/CPA1/2012 (H7N3) cross-protection in vaccinated mice challenged with H7N9 virus. Vaccine 2013;31:4305–13.